# Sand Transport over a Breaker Bar in the Surf Zone

Bart T. Grasmeijer[1] and Leo C. van Rijn[2]

## Abstract

Physical processes related to sand transport under breaking waves and breaker bar behaviour are described on the basis of results of a series of flume experiments. A moderate storm is simulated over a breaker bar profile in the flume. Near the bar crest, the net transport rate between the lowest measurement point and the water surface (measured zone) is dominated by the time-averaged (current-related) transport rate due to the undertow. Outside the bar area, the net transport rate in the measured zone is dominated by the high-frequency (wave-related) transport rate, which is offshore directed due to phase differences between peak orbital velocities and concentrations. Comparison of the measured transport rates and those derived from bed level changes, indicates that the transport rate in a rather thin layer near the sand bed (unmeasured zone), strongly affects the morphological behaviour of the breaker bar. It is expected that in particular the high-frequency transport rate in this unmeasured zone near the bed will dramatically change both the magnitude and direction of the net transport rate.

## Introduction

The nearshore topography of a more or less dissipative beach is often characterized by the presence of one or more breaker-bars parallel to the shoreline. Waves break on these nearshore bars reducing the level of wave energy reaching the shore, in this way acting as a natural breakwater. The morphological behaviour of breaker-bars and the associated net sediment transport rates under the influence of wave action and wave- and tide-induced currents are hardly understood. In this paper the physical processes related to sand transport under breaking waves and breaker bar behaviour are analyzed on the basis of results of a series of flume experiments.

The generation and maintenance of longshore bars is commonly associated with the shoaling and breaking of high-frequency waves and the generation of low-frequency wave effects in the surf zone. Discussions of bar behaviour processes have been given by Greenwood and Davidson-Arnott (1979), by Dean (1973), by

1 Ph.D. student. Institute for Marine and Atmospheric Research Utrecht, Utrecht University, P.O. Box 80.115, 3508 TC Utrecht, the Netherlands, e-mail: B.Grasmeijer@frw.ruu.nl.

2 Sr. Engr., Delft Hydraulics, P.O. Box 177, 2600 MH, Delft, the Netherlands.

Dally (1987), by Holman and Sallenger (1993) and O'Hare and Huntley (1993, 1994).

To demonstrate the relative importance of the various transport processes, in this paper the suspended sediment transport is analyzed in terms of instantaneous and time-averaged quantities. The net transport at height z above the bed can be obtained by time-averaging of the instantaneous values (indicated by an overbar), yielding:

$$\overline{uc} = \bar{u}\,\bar{c} + \overline{\tilde{u}_{high}\tilde{c}_{high}} + \overline{\tilde{u}_{low}\tilde{c}_{low}} \qquad (1)$$

with:

Time-averaged transport (current-related): $\bar{u}\,\bar{c}$ (2)

High-frequency transport (wave-related): $\overline{\tilde{u}_{high} \cdot \tilde{c}_{high}}$ (3)

Low-frequency transport (wave-related): $\overline{\tilde{u}_{low} \cdot \tilde{c}_{low}}$ (4)

The depth-integrated transport rates ($S_{net}$, $S_{average}$, $S_{high}$, $S_{low}$) can be obtained by integration in vertical direction of the components. The physical interpretation of the various transport components is discussed by Van Rijn and Havinga (1995).

### *Experimental set-up*

The experiments were conducted in the Large Research Flume of the Laboratory of Fluid Mechanics of the Faculty of Civil Engineering (Delft University of Technology). The flume has a length of 45 m, a width of 0.8 m and a depth of 1.0 m. Irregular waves (Jonswap spectrum) were generated with a spectrum peak period of $T_p$ = 2.3 s (± 0.2 s).

Two different series of experiments were performed. During the first series of experiments (series A) the sand transport in case of a plane sloping bed (1:100) was studied. In particular, the influence of wave breaking on the suspended sediment transport was studied. Measurements were performed in a measurement section at 18 m from the beginning of the sand bed. The water depth in this section was 0.30 m. The wave height, $H_s$, varied between 0.10 and 0.16 m; the current strength, $U_m$, between 0.0 and 0.30 m/s. Currents were generated in the same direction as the wave propagation.

During the second series of experiments (series B) sediment transport processes related to breaking waves over a breaker bar were examined. The breaker bar is shown in Fig. 3f. The bed profile varies in depth from 0.60 m seawards of the bar to 0.30 m at the bar crest (Fig. 3f). The water depth in the trough landward of the bar crest is 0.50 m. The breaker bar has a steep seaward slope of 1 to 20 and a steep landward slope of 1 to 25. The bed slope landward of the bar trough is 1 to 63. Measurements were performed in 10 different cross-sections along the breaker bar.

For all experiments sand was used with the following grain size characteristics: $D_{10}$ = 0.076 mm, $D_{50}$ = 0.095 mm, and $D_{90}$ = 0.131 mm. The representative (50%) settling velocity of the sediment is $W_s$ = 0.008 m/s. Detailed velocity and concentration data are presented by Grasmeijer and Sies (1995).

A measurement carriage was placed above the flume on which a pump sampler, a wave height meter (WHM), an electro-magnetic fluid velocity meter (EMF), a profile follower (PROFO) and an acoustic sediment transport meter (ASTM) were mounted. The velocities and concentrations were measured at 10 elevations above the bed, the lowest position being about 0.01 m above the crest level of the bed forms. To eliminate small-scale ripple-related variations in velocity and concentration, the measurement carriage was moved forward and backward over a few ripple lengths during the sampling period (5 min.). The velocity of the moving carriage was small (approximately 0.01 m/s) compared to the fluid velocity and large compared to the bed-form migration velocity. A second WHM was placed more landward of the measurement section to check the uniformity of the wave height at the measurement section.

### *Results of plane sloping bed tests*

Shown in Figure 1a are sand concentration profiles for three different wave heights in case of waves superimposed on a current (Um = 0.20 m/s). It can be observed that an increase of the wave height results in an increase of the concentrations and a more uniform concentration profile. Generally, the sediment concentration distribution over vortex ripples shows that the profiles are straight lines in the usual semi-logarithmic plots in which c decays exponentially away from the bed, see Eq.(5).

$$c(z) = c_0 \exp(\frac{-z}{l_s}) \qquad (5)$$

In the present experiments the log-linear region of the concentration profile is found between 0.02 and 0.1 m above mean bed. The concentrations at higher elevations above the bed are larger than may be expected for a log-linear profile. Fig. 1b shows the mixing length ($l_s$) derived from Eq.(6):

$$l_s(z) = [-\frac{d \ln c}{d z}]^{-1} \qquad (6)$$

According to Nielsen (1990), the vertical length scale is closely related to the ripple height r for sharp crested ripples. Osborne and Vincent (1996) found the length scales to be proportional to the ripple height by a factor 2. In Fig. 1b, the vertical length scales in the log-linear region near the bed are about 3 times the bedform height ($l_s \approx 0.035$ m; r ≈ 0.009 to 0.012 m). At higher elevations above the bed (z > 0.1 m), the vertical length scale ($l_s$) increases with the height above the bed. In this region the influence of the bedform on the vertical length scale becomes less pronounced while wave-, current- and breaker-induced mixing become more important.

Figure 1. Concentration profile (A) and mixing length (B) distribution for waves superimposed on a current (Um = 0.20 m/s)

When comparing concentration profiles for different current velocities it appeared that the concentrations in the near bed layer slightly decreased with increasing current velocities while at higher elevations above the bed the concentrations were found to be increasing with increasing current strength. Current-induced mixing

causes according to Van Rijn and Havinga (1995) the increasing concentrations outside the near-bed layer for increasing velocities. They found that the concentrations in the near-bed layer were not noticeably affected by the current velocity increase. Similar results are obtained in the present study.

It is noted that an increasing wave height ($H_s$) from 0 to 0.16 m, which is related to an increase of the fraction of breaking waves ($Q_b$) from 0 to 21%, hardly affects the vertical length scales in the log-linear region of the concentration profile near the bed (Fig.1b), which suggests that breaker-induced mixing is of minor importance in this region.

Nielsen (1984) describes two extremes with respect to breaker-induced mixing. Waves that plunge heavily on shallow bars or on the step of steep beaches can form very strong jets that penetrate right through to the bed and thus introduce very strong external turbulence into the boundary layer itself. Mixing due to bores and spilling breakers has a very different character. Nielsen shows that, in case of monochromatic waves, breaker turbulence changes the upper part of the concentration profile drastically while the lower part is unchanged, so the concentration magnitude and the near-bed vertical length scale ($l_s$) are almost the same under spilling breakers as under non-breaking waves.

In the present experiments the influence of breaking of waves on the concentration profile was observed also, although less pronounced compared to Nielsen. This difference is probably caused by the fact that Nielsen used monochromatic waves for which the fraction of breaking waves is 100%. The fraction of breaking waves in the present experiments is much smaller.

The present data suggest that the mixing effect of spilling breakers might be of importance in case of relatively small breaking waves ($H_s/h < 0.5$) in the presence of no or weak current ($U_m < 0.1$ m/s), especially in the upper part of the concentration profile ($z/h > 0.33$). In case of a larger wave height and/or a stronger current the suspended sediment distribution is predominantly determined by wave- and current-induced mixing, despite the sometimes-larger fraction of breaking waves. The effect of breaker-induced mixing is relatively small.

To get a better insight in the relationship between the transport rate and the fraction of breaking waves an empirical formula was fitted to the present data, expressing the depth-integrated time-averaged transport rate as a function of the mean velocity, the relative wave height, the peak near-bed velocities and the fraction of breaking waves ($Q_b$). From the empirical formula (with a regression coefficient of 0.99) it appeared that the influence of spilling breakers on the depth-integrated transport rate is moderate. The depth-integrated transport rate was found to be roughly proportional to $(1-Q_b)^{-1}$, see Fig. 2. For example, an increase of $Q_b$ from 0 to 30% leads to an increase of the depth-integrated transport rate of approximately 40%. In comparison, the increase of the relative wave height related to these values of $Q_b$ leads to an increase of the transport rate of more than 170%.

Figure 2. Influence of fraction of breaking waves on time-averaged transport rate.

### *Results of breaker bar tests*

Wave height, fraction of breaking waves and transport rates are presented in Fig. 3 as a function of the location in the flume. It can be observed that waves are shoaling towards the bar crest (Fig.3a). Maximum wave height is found near the bar crest. Moving further landwards, the wave height decreases both due to the increasing water depth and due to energy dissipation caused by breaking of waves. Nearly all breaking waves were of the spilling breaker type. Occasionally near the bar crest, a plunging breaker occurred. It is interesting to note that the fraction of breaking waves is largest just landward of the bar crest (Fig.3b). Breaking waves of the spilling breaker type start breaking near the bar crest but continue breaking over several wave lengths while propagating further landwards. Thus, waves initially breaking near the bar crest are also included in the fraction of breaking waves more landward of the crest.

The depth-integrated transport rates calculated from velocity and concentration measurements are compared with transport rates measured from bed profile changes over short time intervals (Fig.3c-e). In contrast with Van Rijn and Havinga (1995), the transport rates calculated from velocity and concentration measurements were not extrapolated to the unmeasured zone between the lowest measuring point and the mean bed level. Thus, the calculated depth-integrated values represent the suspended transport rather than the total transport rates (bed-load transport excluded).

Figure 3. Transport rates along the breaker bar

From Fig. 3c it can be observed that the net suspended transport rate, $S_{net}$, is offshore directed in all measurement sections and increasing when moving towards the bar crest. Decreasing transport rates are found when moving further landwards. Although the same trends can be observed for the time-averaged suspended transport rate ($S_{average}$, Fig. 3c), occasionally small transport rates were found to be onshore directed as a result from the time-averaged velocity near the bed being onshore directed (Longuet-Higgins streaming) and the sediment not being stirred up to high elevations above the bed where the time-averaged velocity is offshore directed (return flow or undertow).

The high-frequency suspended transport rate ($S_{high}$) is found to be offshore directed in all measurement sections (Fig. 3d) and increasing when moving toward the bar crest where the largest high-frequency suspended transport rates are found. Moving further landwards a pronounced decrease of $S_{high}$ can be observed. The high-frequency suspended transport rate is found to be negligible in the measurement sections landward of the bar, where the fraction of breaking waves is largest. The offshore direction of the high-frequency suspended transport rate is likely to be related to the mechanism of sand suspension over rippled bed forms. From the analysis of the concentration signals and from visual observations it appeared that, on the time scale of a single wave cycle, sediment was eroded from the bed at the onshore stroke of the wave and mobilized in vortices between the ripples. At flow reversal from on- to offshore direction the vortex cloud was lifted and advected leading to high concentrations at the offshore stroke of the wave.

This variation in timing of concentration maxima and minima results in a vertical distribution in which the high-frequency transport rate tends to be onshore directed near the bed and offshore directed at higher elevations above the bed. Measurements close to the bed could not be made. Hence, the transport rate in the near bed layer (bed-load transport) could not be estimated from the data, but this transport rate is believed to be onshore directed.

From Fig. 3d it can be observed that in the measurement locations just landward of the bar crest, the low-frequency suspended transport rate is found to be relatively large and offshore directed. In these measurement sections the low-frequency suspended transport rates may not only be caused by the bound-long wave phenomenon. The undertow generated by irregular breaking waves may also show long-period velocity oscillations. Large concentration magnitudes under high-amplitude waves combined with the undertow oscillations induced by breaking waves results in a relatively large offshore-directed low-frequency suspended transport rate at locations just landward of the bar crest.

The wave-related suspended transport is dominated by the high-frequency component in nearly all measurement locations seaward of the breaker bar. At locations just landward of the bar crest, however, the low-frequency suspended transport rate exceeds the high-frequency component. It is interesting to note that the dominance of $S_{low}$ over $S_{high}$ occurs at locations were the fraction of breaking waves is relatively large, indicating that long period oscillations of the undertow are important.

Transport rates based on morphological changes were determined by measuring the bed level at the flume window every 0.25 m along the profile. In Fig. 3f the initial bed level and the bed level after 9700 s of wave action are plotted for series B2. It can be observed that morphological changes take place especially at the seaward slope of the bar (accretion), and at the landward slope of the bar (erosion). The bar crest is moving seawards. Transport rates were calculated from the bed level changes assuming that the transport rates at deep water seaward of the bar are zero. Transport rates based on these morphological changes ($S_{morphology}$) are plotted in Fig. 3e, as well as the time-averaged net suspended transport rates based on instantaneous velocity and concentrations measurements ($S_{net}$) and the difference between both curves ($S_{rest}$). The $S_{net}$-value is the same curve as shown in Fig. 3c. It can be observed from Fig. 3e that $S_{morphology}$ is onshore directed landward of the bar and offshore directed near the bar crest. At locations near the bar crest $S_{net}$ and $S_{morphology}$ are both found to be offshore directed. The rest term, $S_{rest}$, is onshore directed in nearly all measurement locations. Largest values are found at locations near the bar crest, while $S_{rest}$ is negligible in the measurement section where the fraction of breaking waves is largest.

It is noted that the transport rates derived from the bed-level changes ($S_{morphology}$) represents both the suspended and the bed load transport rate, whereas the transport rates derived from the velocity and concentration measurements ($S_{net}$) only represents the suspended transport.

The discrepancy between the transport rate based on morphology and that based on velocity and concentration measurements probably represents a combination of

wave-related transport and current-related transport in the unmeasured zone near the bed. From analysis of the vertical distribution of transport rates it appeared that in particular the high-frequency wave-related transport rate near the bed tends to be onshore directed. The relatively large high-frequency velocities with onshore near-bed peak velocities larger than offshore near-bed peak velocities, together with the large concentrations magnitudes (and variation in concentration) may lead to large high-frequency transport rates in onshore direction. It is expected that the high-frequency transport rate in the unmeasured zone near the bed will dramatically change both the magnitude and the direction of the total net transport rate.

## Conclusions

The main findings of the study are summarized in the following conclusions:

- The effect of the fraction of breaking waves ($Q_b$) on the depth-integrated and time-averaged (mean) transport rate was found to be relatively small. An increase of $Q_b$ from 0 to 30% gave an increase of the transport rate by about 40%.
- Near the bar crest, the net transport in the measured zone is dominated by the time-averaged (current-related) transport rate due to the undertow.
- Outside the bar area, the net transport in the measured zone is dominated by the high-frequency (wave-related) transport rate, which is offshore directed due to phase differences between peak orbital velocities and concentrations.
- With the exception of the region just landward of the bar crest, where the fraction of breaking waves is relatively large, the low-frequency transport rate is negligible.
- The morphological behaviour of a breaker bar and the associated net transport rates are strongly related to the wave-related transport rates in a rather thin layer near the sediment bed.
- Measurement of instantaneous velocities and concentrations in this layer are of crucial importance to determine the net transport rates and hence the net migration rate of the bar. It is, however, hardly possible to measure these transport rates with the available measurement techniques, not even in flume conditions.

## Acknowledgments

The present study was a joint project of Delft Hydraulics, Delft University of Technology, Rijkswaterstaat of the Dutch Ministry of Public Works and the MAST-program of the EEC.

## References

***Dally, W.R. (1987).*** *"Longshore bar formation - surf beat or undertow ?". Proceedings of Coastal Sediments '87, pp. 71-85.*

***Dean, R.G. (1973).*** *"Heuristic models of sand transport in the surf zone". Conf. on Eng. Dynamics in Coastal Zone". Sydney, Australia.*

***Grasmeijer, B.T. and Sies, E.M. (1995).*** *"Sediment concentrations and sediment transport in case of irregular breaking waves over a plane sloping bed and a*

*barred profile". Part H and I. Delft Hydr., Delft Univ. of Technol., Coastal Eng. Dep., Delft, The Netherlands.*

***Grasmeijer, B.T. (1996).*** *"Sediment concentrations and transport in case of irregular breaking waves and currents over plane and barred profiles". Part J and K. . Delft Hydr., Delft Univ. of Technol., Coastal Eng. Dep., Delft, The Netherlands*

***Greenwood, B. and Davidson-Arnott, R.G.D. (1979).*** *"Sedimentation and equilibrium in wave-formed bars: a review and case study". Canadian Journal of Earth Sc., Vol. 16, pp. 312-332*

***Holman, R.A. and Sallenger, A.H. (1993).*** *"Sand bar generation: a discussion of the Duck experiment series". Journal of Coastal Research, SI 15, pp. 76-92.*

***Longuet-Higgens, M.S., 1953.*** *"Mass transport in water waves". Royal Society Phil. Trans., London, Vol. 245, A903, pp. 535-581.*

***O'Hare, T.J. and Huntley, D.A. (1994).*** *"Bar formation due to wave groups and associated long waves". Marine Geology, Vol. 116, pp. 313-325.*

***O'Hare, T.J. and Huntley, D.A. (1993).*** *"Sand bar evolution beneath partially-standing waves: laboratory experiments and model simulations". Continental Shelf Research. Vol.13, No.11, pp. 1149-1181.*

***Osborne, P.D. and Vincent, C.E. (1996).*** *"Vertical and horizontal structure in suspended sand concentrations and wave-induced fluxes over bedforms". Marine Geology, Vol. 131, pp. 195-208*

***Van Rijn, L.C. and Havinga, F.J. (1995).*** *"Transport of fine sands by currents and waves". Journal of Waterway, Port, Coastal and Ocean Engineering, Vol. 121, No. 2, pp. 123-133.*

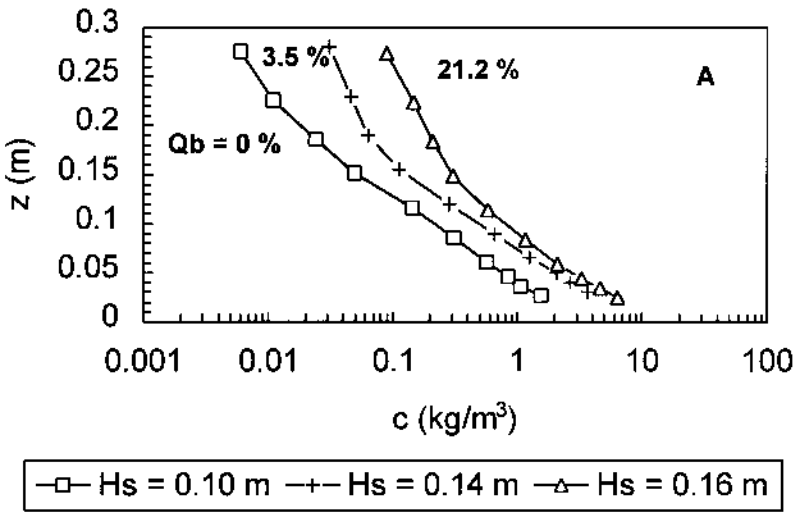
0.3
0.25
0.2
0.15
0.1
0.05
0
z (m)
3.5 %
21.2 %
A
Qb = 0 %
0.001
0.01
0.1
1
10
100
c (kg/m3)
Hs = 0.10 m
Hs = 0.14 m
Hs = 0.16 m

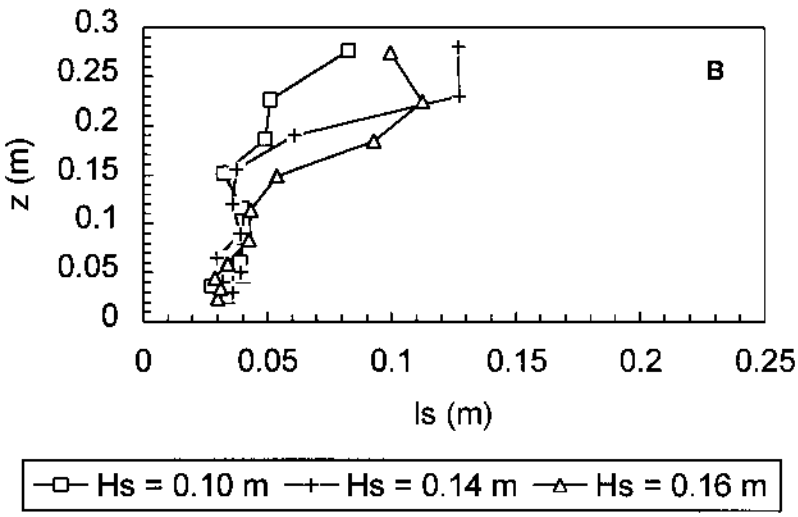
0.3
0.25
0.2
0.15
0.1
0.05
0
z (m)
B
0
0.05
0.1
0.15
0.2
0.25
ls (m)
Hs = 0.10 m
Hs = 0.14 m
Hs = 0.16 m

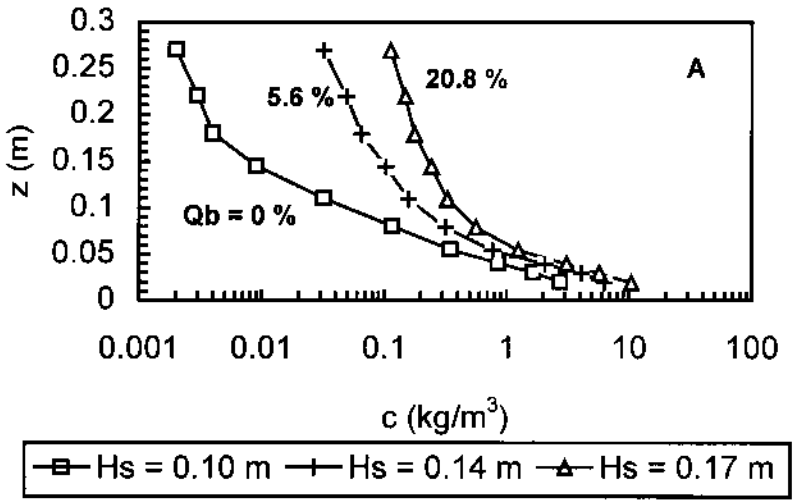
0.3
0.25
0.2
0.15
0.1
0.05
0
z (m)
A
20.8 %
5.6 %
Qb = 0 %
0.001
0.01
0.1
1
10
100
c (kg/m3)
Hs = 0.10 m
Hs = 0.14 m
Hs = 0.17 m

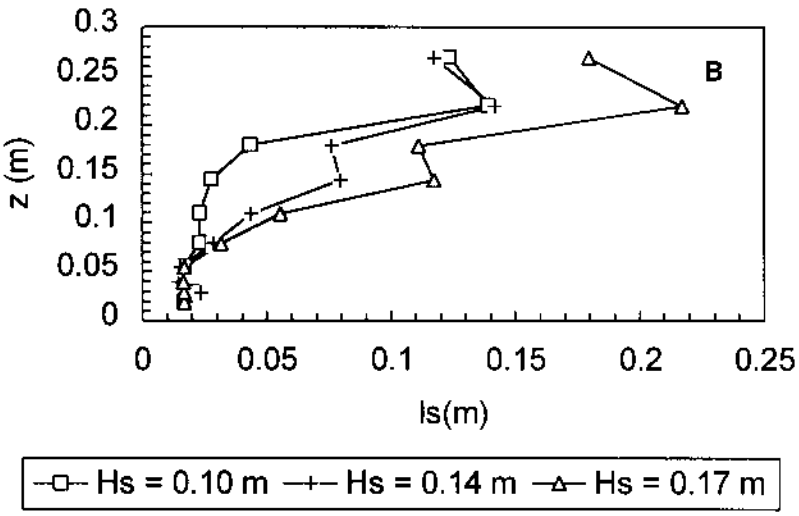
0.3
0.25
0.2
0.15
0.1
0.05
0
z (m)
B
0
0.05
0.1
0.15
0.2
0.25
ls(m)
Hs = 0.10 m
Hs = 0.14 m
Hs = 0.17 m

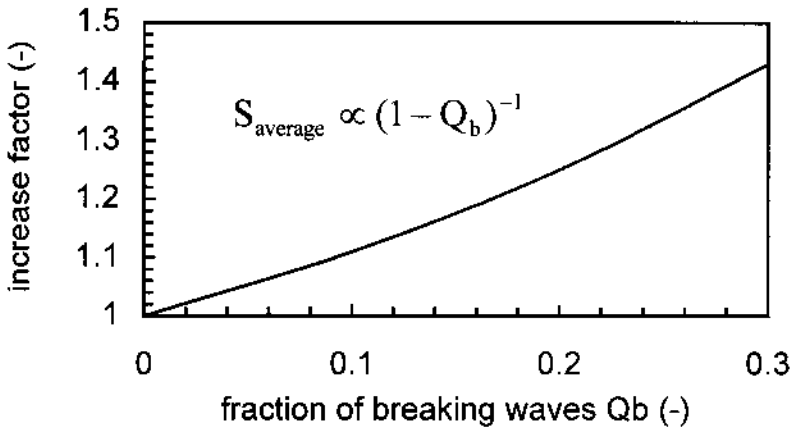
1.5
1.4
1.3
1.2
1.1
1
increase factor (-)
$S_{average} \propto (1 - Q_b)^{-1}$
0
0.1
0.2
0.3
fraction of breaking waves Qb (-)